UC Irvine
UC Irvine Previously Published Works

Title

High purity specimens of URu2Si2 produced by a molten metal flux technique

Permalink

https://escholarship.org/uc/item/5vm201w5

Authors

Baumbach, RE
Fisk, Z
Ronning, F
et al.

Publication Date

2014-11-22

DOI

10.1080/14786435.2014.895876

Copyright Information

Peer reviewed

Taylor & Francis
Taylor & Francis Group

High purity specimens of URu_2Si_2 produced by a molten metal flux technique

R.E. Baumbach[a]*, Z. Fisk[b], F. Ronning[a], R. Movshovich[a], J.D. Thompson[a] and E.D. Bauer[a]

[a] *MPA-CMMS Los Alamos National Laboratory, Los Alamos, NM 87545, USA;* [b] *Department of Physics, University of California, Irvine, CA 92697, USA*

We report a molten metal flux technique to produce high purity specimens of URu_2Si_2. Magnetic susceptibility ($M/H = \chi$), heat capacity (C) and electrical resistivity (ρ) measurements show that the bulk properties of these crystals are similar to those that are produced by the Czochralski technique followed by solid-state electro-transport. In particular, we find residual resistivity ratios RRR $= \rho_{300K}/\rho_0$ as large as 220.

Keywords: crystal growth; superconducting materials; strongly correlated electrons

1. Introduction

For nearly three decades, URu_2Si_2 has been a central topic in the field of strongly correlated electrons, due to the fact that it exhibits two robust mean field second-order phase transitions: one at the "hidden order" temperature $T_0 \approx 17.5$ K and another at the superconducting phase transition $T_c \approx 0.8$–1.4 K [1–3]. The hidden order transition is given its name because, although roughly 0.2Rln2 of entropy is released at T_0 (clearly showing a phase transition to a new state for $T \leq T_0$), intense experimental and theoretical efforts to uncover the order parameter have been unsuccessful: e.g. neutron scattering and μSR techniques yield ordered moments that are much too small to account for the entropy that is released at T_0 [4,5]. Considerable interest has also been paid to the superconducting state, which is clearly unconventional as evidenced by: (1) its occurrence deep inside the hidden order state [1–3], (2) the low carrier density from which it emerges [6,7], (3) the large upper critical field [8] and (4) measurements which suggest the presence of nodes in the superconducting energy gap [7,9–11]. Furthermore, a variety of studies have shown that magnetism is found on the border of the hidden order state. For instance, measurements under applied pressure show that at $P_c \approx 0.5$ GPa, there is a first-order phase transition from hidden order to conventional antiferromagnetism, which is accompanied by destruction of the superconductivity [12–14]. Similar behaviour is observed with chemical pressure in the substitution series $URu_{2-x}Fe_xSi_2$ [15]. For these and other reasons, the effort to understand URu_2Si_2 remains an active field of research.

*Corresponding author. Email: edbauer@lanl.gov

Many of the recent advances in understanding URu_2Si_2 stem from the relationship between advanced measurement techniques and improved sample quality. Regarding sample quality, it was recently recognized that ultra high purity specimens with residual resistivity ratios RRR $= \rho_{300K}/\rho_0 \approx$ 100–1000 can be produced by synthesizing a single crystal using the Czochralski technique, followed by solid-state electro-transport (also referred to as "electrorefining") [16,17]. This is in contrast to "as-grown" samples that are produced by the Czochralski technique, where RRR $\approx$ 10 (e.g. see [14,18]).

An early benefit to studying high purity specimens was the resolution of a long-standing question relating to the coexistence of the hidden order phase and small moment antiferromagnetism at $P = 0$. Systematic studies of crystals with different RRR have shown that the small moment antiferromagnetism is likely due to internal strain, which produces rare regions of antiferromagnetism which are analogous to what is seen for $P \geq P_c$ (e.g. see [19]). Measurements of high purity specimens have also driven investigations of the Fermi surface which, surprisingly, shows little change as the ground state is driven from hidden order to antiferromagnetism as a function of pressure [6,20–22]. High quality specimens have also been essential for sensitive measurements such as STM [23,24] and ARPES [25]. In fact, the influence of sample purity is even reflected in bulk measurements such as electrical resistivity, where T_c, T_0 and the power law dependence of $\rho(T)$ at low temperatures are all related to RRR [17]. Therefore, it is clear that investigation of high purity specimens is essential to develop an understanding of this compound. However, present synthesis techniques severely limit access to quality specimens.

Herein, we report a new molten metal flux technique to produce high purity specimens of URu_2Si_2. Our initial investigation reveals that it is possible to routinely produce single-crystal platelets where RRR is as large as 220. We report magnetic susceptibility, heat capacity and electrical resistivity measurements which demonstrate that the bulk properties of these crystals are comparable to those that are produced by the Czochralski technique followed by solid-state electro-transport. We expect that this growth technique will expand access to high quality URu_2Si_2, and may thereby accelerate progress towards an understanding of this material.

2. Experimental details

Single crystals of URu_2Si_2 were grown from elements with purities >99.9% in a molten In flux. The reaction ampoules were prepared by loading the elements into a 5 cm^3 tantalum crucible in the ratio 1(U):2(Ru):2(Si):22(In). The crucible was then loaded into an alumina tube spanning the bore of a high temperature vertical furnace. Ultra high purity argon gas was passed through the tube and a zirconium getter was placed in a pot above the tantalum crucible in order to purify the argon at high temperatures. The crucible was then heated to 1400°C at 70°C/hr, held at this temperature for 10 h and quickly cooled to room temperature at an average rate of 100 C/hr. The indium flux was subsequently removed using hydrochloric acid, to which the URu_2Si_2 crystals are impervious. This technique produced single crystal *ab-plane* platelets similar to the one shown in Figure 1.

Magnetization $M(T, H)$ measurements were carried out for a mosaic of single crystals for temperatures $T = 1.8$–350 K under an applied magnetic field of $H = 1$ kOe applied parallel to the c-axis using a Quantum Design Magnetic Property Measurement System. The specific heat $C(T, H)$ was measured for a mosaic of single crystals for $T = 0.3$–30 K using a Quantum Design Physical Property Measurement System. The electrical resistivity

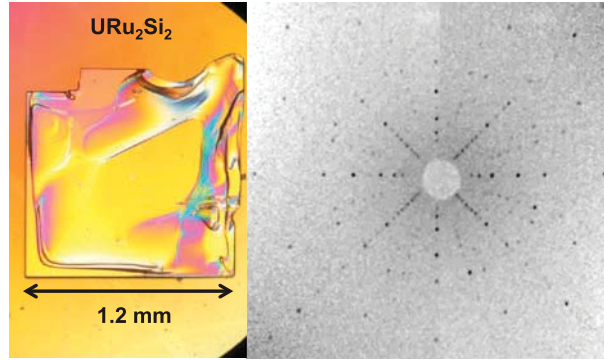Figure 1. (colour online) (a) An image of a typical URu_2Si_2 single crystal taken under a Nomarski polarized light filter. (b) A Laue backscatter image of a single crystal of URu_2Si_2 which reveals that the *c*-axis is perpendicular to the plate face.

$\rho(T, H)$ was measured for $T = 0.4$–300 K up to $H = 90$ kOe for perpendicular ($\perp$) to the *c*-axis and up to 17.5 kOe for H parallel ($\parallel$) to the *c*-axis using a Quantum Design Physical Property Measurement System.

3. Results

Shown in the left panel of Figure 1 is a typical single crystal platelet of URu_2Si_2, for which the dimensions are ∼1.2 mm length and ∼0.05 mm thickness. The image was taken using a Nomarski polarized light filter, where the lack of texture on the flat surfaces suggests minimal surface strain. In the right panel of Figure 1, we show a Laue backscatter image which reveals that the crystals form with the *c*-axis perpendicular to the plate surface.

In Figure 2(a), we show the magnetic susceptibility $\chi(T) = M(T)/H$ with a magnetic field $H = 1$ kOe applied $\parallel$ to the *c*-axis. As expected, $\chi(T)$ increases with decreasing T for $T < 350$ K and evolves through a maximum near 50 K. For 100 K $\leq T \leq 350$ K, $\chi(T)$ exhibits Curie-Weiss behaviour given by the expression,

$$\chi = \chi_0 + C/(T - \Theta) \tag{1}$$

where $\chi_0 = 0.0013$ cm³/mol, $\Theta = -59$ K and $\mu_{eff} = 3.1$ μ_B. The values for θ and μ_{eff} are comparable to those found in previous reports [1]. As shown in Figure 2(b), $\chi(T)$ is abruptly reduced at the hidden order temperature $T_{HO} \approx 17.5$ K. For $T \leq 12$ K, $\chi(T)$ shows a weak upturn with decreasing T. In Figure 2(c), we show the evolution of $M(H)$ at $T = 2$ K, which is consistent with previous results.

The heat capacity divided by temperature C/T vs. T data, taken for a mosaic of single crystals, are shown in Figure 3(a). Again, we see behaviour that is characteristic of high quality specimens of URu_2Si_2. The hidden order temperature is found near $T_{HO} \approx 17.5$ K, with a width $\Delta T_{HO} = 0.6$ K (Figure 3(b)). The entropy under the HO transition is comparable to results for crystals prepared using other techniques. The superconducting transition occurs near $T_c \approx 1.3$ K, with a width $\Delta T_c = 0.4$ K (Figure 3(c)). We also find that C/T gradually increases with decreasing T for $T_c \leq T \leq 7$ K.

Electrical resistivity ρ vs. T data for a representative single-crystal specimen are presented in Figure 4(a), where the current is applied in the ab plane. $\rho(T)$ initially
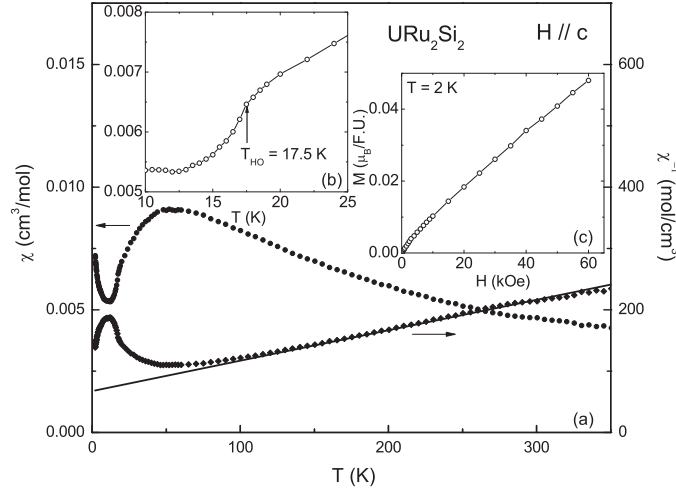
Figure 2. (a) Magnetic susceptibility $\chi = M/H$ and the inverse magnetic susceptibility χ^{-1} vs. temperature T for a mosaic of URu_2Si_2 single crystals where the magnetic field $H = 1$ kOe was applied parallel to the *c*-axis. (b) $\chi(T)$ in the temperature range surrounding the hidden order transition T_{HO}. (c) The magnetization M vs. H at $T = 2$ K.
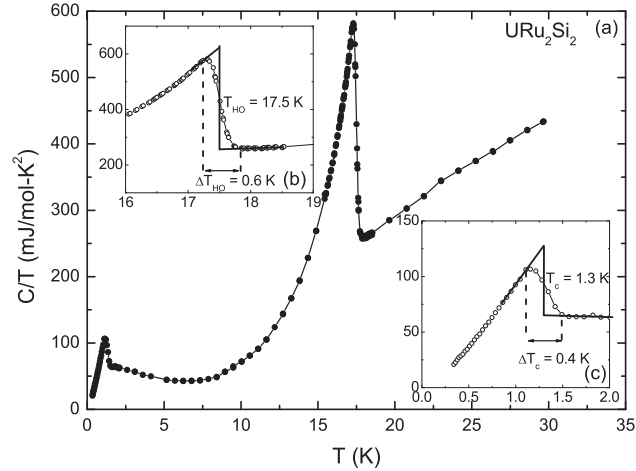

Figure 3. (a) Heat capacity divided by temperature C/T vs. T for a mosaic of URu_2Si_2 single crystals. (b) C/T in the vicinity of the hidden order transition T_{HO}. (c) C/T near the superconducting transition T_c.

increases with decreasing temperature and evolves through a maximum near the coherence temperature at 82 K. The resistivity then drops quickly until the hidden order transition opens a gap which results in an anomaly near $T_{HO} \approx 17.8$ K with a width of $\Delta T_{HO} \approx 0.44$ K, as shown in Figure 4(b). Following the hidden order transition, the resistivity falls towards 2 $\mu\Omega$cm near 1.5 K. We perform a fit to the data for 1.5 K $\leq T \leq 15$ K using the expression,
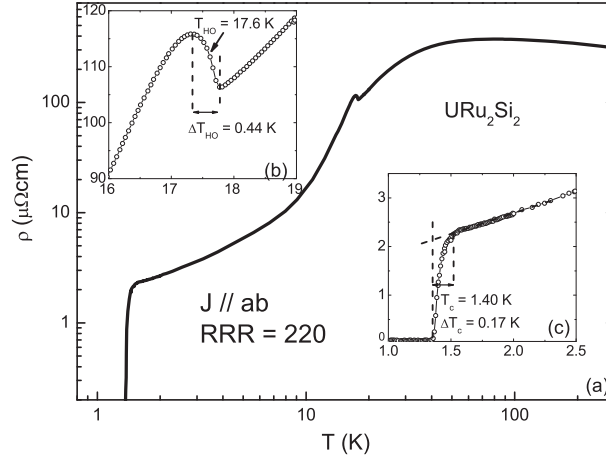
$$\rho(T) = \rho_0 + AT^x + B\exp(-\Delta/\text{T}) \tag{2}$$

Figure 4. (a) Electrical resistivity ρ vs. temperature T for a representative single crystal of URu$_2$Si$_2$ where the current is applied in the ab plane. (b) $\rho(T)$ in the vicinity of the hidden order transition T_{HO}. (c) $\rho(T)$ in the vicinity of the superconducting transition T_c.

where $\rho_0 = 1.37\,\mu\Omega$cm is the residual resistivity at zero temperature, $A = 0.51\mu\Omega$cm/K^n is the coefficient of the power law behaviour, $n = 1.35$ is the power law exponent, $B = 7823\,\mu\Omega$cm is the coefficient of the exponential behaviour and $\Delta = 77$ K is the gap size. These fit parameters are in good agreement with earlier results on UHP samples [17]. From the value of ρ_0, we estimate that RRR = 220 for this specimen. Throughout the batch, we find that RRR ranges from 50 to 220. Finally, we observe a superconducting transition at $T_c = 1.4$ K with a transition width $\Delta T_c = 0.17$ K (Figure 4(c)).

In Figure 5, we show $\rho(T)$ near T_c under applied magnetic fields for H parallel and perpendicular to the c-axis. As expected, T_c is suppressed with increasing H. We plot the field dependence of T_c for each direction in Figure 6. Here, T_c is defined as the temperature where $\rho(T)$ falls to 50% of the normal state value just above the transition. The transition width, illustrated as bars, is defined as the temperature where $\rho(T)$ falls 10 and 90% of the normal state value. We also show the temperature where $\rho(T)$ falls to zero. Another important feature of the data shown in Figure 5 is that $\rho(T)$ increases strongly with increasing H. This behaviour has been observed previously and is related to the fact that URu$_2$Si$_2$ is a compensated electron-hole semimetal, for which $\Delta\rho(H)/\rho_0$ is proportional to H^2 [7].

We next consider the initial slopes of $H_{c2}(T)$ near T_c, where we find $(\partial H_{c2}(T)/\partial T)_{Tc} = -45\,$kOe/K and $-130\,$kOe/K for $H\ \parallel$ and $\perp$ c, respectively. These values are similar to those previously observed for URu$_2$Si$_2$ [8]. From these values, we calculate the Ginzburg–Landau coherence lengths parallel and perpendicular to the ab-plane, ξ_{abs} and ξ_c, respectively, using the expressions [26],

$$\left(dH_{c2}^{\parallel,c}/dT\right)_{T_c} = -\Phi_0/2\pi T_c\xi_{ab}^2 \qquad (3)$$

and

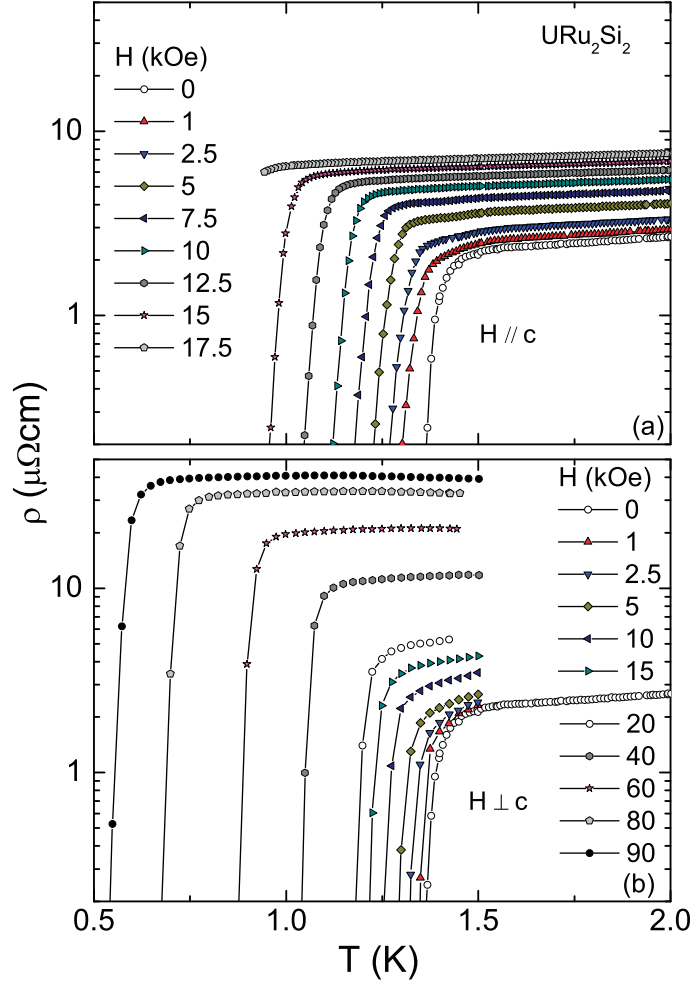$$\left(dH_{c2}^{\perp,c}/dT\right)_{T_c} = -\Phi_0/2\pi T_c\xi_{ab}\xi_c, \qquad (4)$$

Figure 5. (colour online) (a) Electrical resistivity ρ vs. temperature T under magnetic fields H applied parallel ($\parallel$) to the c-axis. (b) $\rho(T)$ for H applied perpendicular ($\perp$) to the c-axis.

where $\Phi_0 = 2.07 \times 10^{-7}$ Gcm^2 is the flux quantum. From the values $(dH_{c2}^{\parallel-c}/dT)_{T_c} = -45$ kOe/K and $(dH_{c2}^{\perp-c}/dT)_{T_c} = -130$ kOe/K, we obtain $\xi_{ab} = 72$ Å and $\xi_c = 25$ Å. We also apply the expression,

$$\xi = 0.18 \hbar v_F / k_B T_c, \tag{5}$$

where $\hbar$ is the Planck constant, k_B is the Boltzmann constant, and $v_{F,ab} = 7.4 \times 10^5$ cm/s and $v_{F,c} = 2.6 \times 10^5$ cm/s are the Fermi velocities calculated from ξ_{ab} and ξ_c, respectively. The values that we find for ξ and v_F are consistent with earlier results [2,18].

In Figure 7, we plot the hidden order and superconducting transition temperatures, T_{HO} and T_c, vs. RRR for several representative samples that were grown using the molten indium flux growth technique described above. For comparison, we also plot these quantities for single-crystal specimens that were prepared using the Czochralski technique, where those
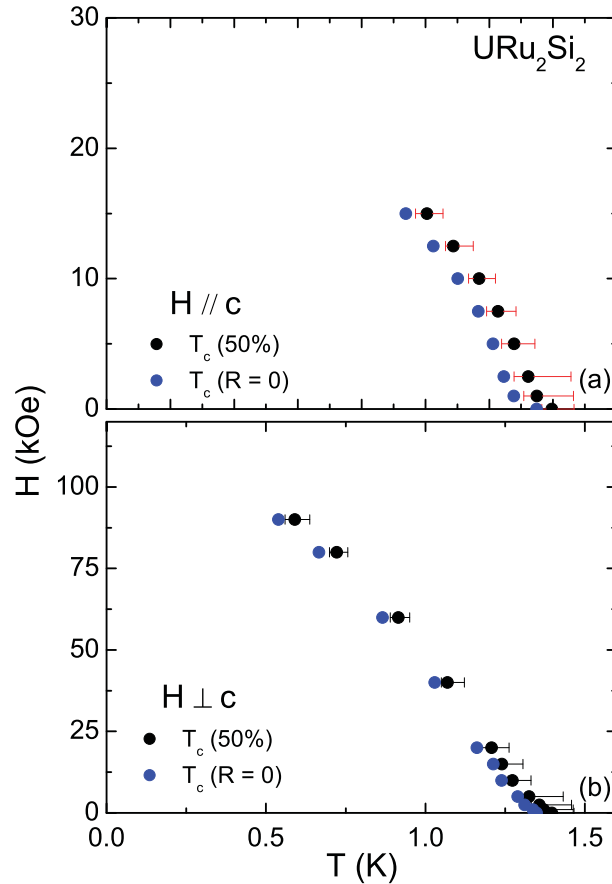
Figure 6. (colour online) (a) The upper critical field H_{c2} vs. temperature T for H applied parallel (∥) to the c-axis. The method to define T_c is given in the text. $H_{c2}(T)$ for H applied perpendicular (⊥) to the c-axis.

with large RRR were post-processed by electrorefining. Here, we see that T_{HO} and T_c follow the same trends for other high purity specimens, further supporting the point of view that these samples are comparable to those that are produced by Czochralski followed by electrorefining, and should be described as being ultra high purity.

4. Summary

We have demonstrated a molten indium flux technique to produce high quality specimens of URu_2Si_2. Crystals grown by this technique show RRR = 50–220, which is a significant improvement over what is typically found for single crystals grown using the Czochralski technique without post-processing by zone refinement. In fact, RRR for the flux grown crystals approaches that of zone refined Czochralski grown samples. We have shown that the bulk properties of the flux grown samples (i.e. magnetic susceptibility, heat capacity and electrical resistivity) are consistent with earlier results for such high purity samples.
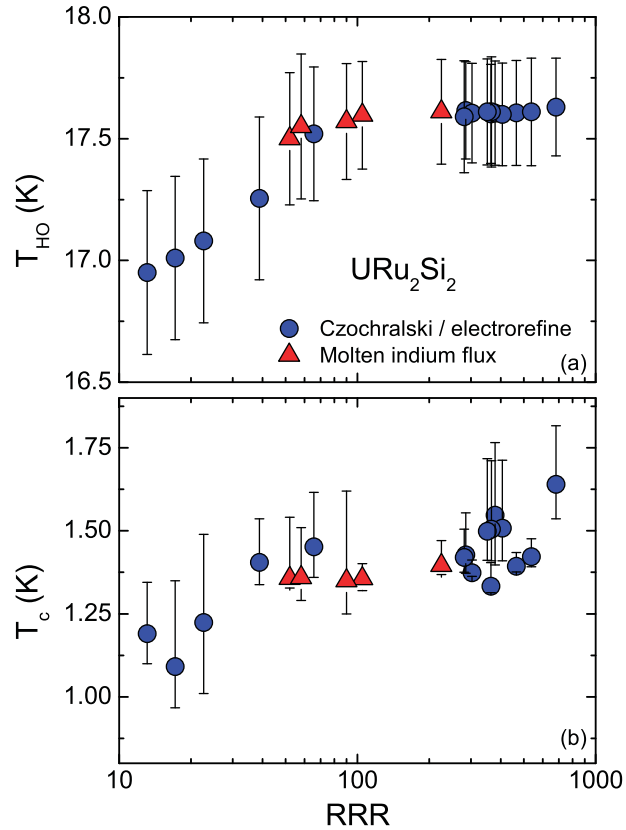
Figure 7. (colour online) Comparison between ultra high purity URu_2Si_2 crystals grown by the Czochralski technique followed by electrorefining (blue circles) and those that were produced in a molten indium flux (red triangles) (a) Dependence of the hidden order transition temperature T_{HO} on the residual resistivity ratio RRR $= \rho_{300K}/\rho_0$, where RRR is defined as described in the text. The bars represent the transition width (see Figure 4(b)). (b) Dependence of the superconducting transition temperature T_c on RRR. The bars represent the transition width, as defined in the text.

Therefore, since the technique reported here relies only on equipment that is readily available in many synthesis laboratories, we expect that it will expand access to high quality URu_2Si_2, and may thereby accelerate progress towards an understanding of this material.

Acknowledgements

References

[1] T.T.M. Palstra, A.A. Menovsky, J. van den Berg, A.J. Dirkmaat, P.H. Kes, G.J. Nieuwenhuys and J.A. Mydosh, Phys. Rev. Lett. 55 (1985) p.2727.

[2] W. Schlabitz, J. Baumann, B. Pollit, U. Rauchschwalbe, H.M. Mayer, U. Ahlheim and C.D. Bredl, Z. Phys. B 62 (1986) p.171.

[3] M.B. Maple, J.W. Chen, Y. Dalichaouch, T. Kohara, C. Rossel, M.S. Torikachvili, M.W. McElfresh and J.D. Thompson, Phys. Rev. Lett. 56 (1986) p.185.

[4] C. Broholm, J.K. Kjems, W.J.L. Buyers, P. Matthews, T.T.M. Palstra, A.A. Menovsky and J.A. Mydosh, Phys. Rev. Lett. 58 (1987) p.1467.

[5] D.E. MacLaughlin, D.W. Cooke, R.H. Heffner, R.L. Hutson, M.W. McElfresh, M.E. Schillaci, H.D. Rempp, J.L. Smith, J.O. Willis, E. Zirngiebl, C. Boekema, R.L. Lichti and J. Oostens, Phys. Rev. B 37 (1988) p.3153.

[6] H. Ohkuni, Y. Inada, Y. Tokiwa, K. Sakurai, R. Settai, T. Honma, Y. Haga, E. Yamamoto, Y. Onuki, H. Yamagami, S. Takahashi and T. Yanagisawa, Phil. Mag. B 79 (1999) p.1045.

[7] Y. Kasahara, T. Iwasawa, H. Shishido, T. Shibauchi, K. Behnia, Y. Haga, T.D. Matsuda, Y. Onuki, M. Sigrist and Y. Matsuda, Phys. Rev. Lett. 99 (2007) p.116402.

[8] W.K. Kwok, L.E. DeLong, G.W. Crabtree, D.G. Hinks and R. Joynt, Phys. Rev. B 41 (1990) p.11649.

[9] K. Hasselbach, J.R. Kirtley and J. Flouquet, Phys. Rev. B 47 (1993) p.509.

[10] Y. Kohori, K. Matsuda and T. Kohara, J. Phys. Soc. Jpn. 65 (1996) p.1083.

[11] K. Yano, T. Sakakibara, T. Tayama, M. Yokoyama, H. Amitsuka, Y. Homma, P. Miranovic, M. Ichioka, Y. Tsutsumi and K. Machida, Phys. Rev. Lett. 100 (2008) p.017004.

[12] M.W. McElfresh, J.D. Thompson, J.O. Willis, M.B. Maple, T. Kohara and M.S. Torikachvili, Phys. Rev. B 35 (1987) p.43.

[13] H. Amitsuka, M. Sato, N. Metoki, M. Yokoyama, K. Kuwahara, T. Sakakibara, H. Morimoto, S. Kawarazaki, Y. Miyako and J.A. Mydosh, Phys. Rev. Lett. 83 (1999) p.5114.

[14] J.R. Jeffries, N.P. Butch, B.T. Yukich and M.B. Maple, J. Phys. Condens. Matter 20 (2008) p.095225.

[15] N. Kanchanavatee, M. Janoschek, R.E. Baumbach, J.J. Hamlin, D.A. Zocco, K. Huang and M.B. Maple, Phys. Rev. B 84 (2011) p.245122.

[16] T.D. Matsuda, D. Aoki, S. Ikeda, E. Yamamoto, Y. Haga, H. Ohkuni, R. Settai and Y. Onuki, J. Phys. Soc. Jpn. Suppl. A 77 (2008) p.362.

[17] T.D. Matsuda, E. Hassinger, D. Aoki, V. Taufour, G. Knebel, N. Tateiwa, E. Yamamoto, Y. Haga, Y. Onuki, Z. Fisk and J. Flouquet, J. Phys. Soc. Jpn. 80 (2011) p.114710.

[18] T.T.M. Palstra, A.A. Menovsky and J.A. Mydosh, Phys. Rev. B 33 (1986) p.6527.

[19] J.A. Mydosh and P.M. Oppeneer, Rev. Mod. Phys. 83 (2011) p.1301.

[20] E. Hassinger, G. Knebel, T.D. Matsuda, D. Aoki, V. Taufour and J. Flouquet, Phys. Rev. Lett. 105 (2010) p.216409.

[21] M.M. Altarawneh, N. Harrison, S.E. Sebastian, L. Balicas, P.H. Tobash, J.D. Thompson, F. Ronning and E.D. Bauer, Phys. Rev. Lett. 106 (2011) p.146403.

[22] D. Aoki, G. Knebel, I. Sheikin, E. Hassinger, L. Malone, T.D. Matsuda and J. Flouquet, J. Phys. Soc. Jpn. 81 (2012) p.074715.

[23] P. Aynajian, E.H. da Silva Neto, C.V. Parker, Y. Huang, A. Pasupathy, J. Mydosh and A. Yazdani, Proc. Natl. Acad. Sci. 107 (2010) p.10383.

[24] A.R. Schmidt, M.H. Hamidian, P. Wahl, F. Meier, A.V. Balatsky, J.D. Garrett, T.J. Williams, G.M. Luke and J.C. Davis, Nature 465 (2010) p.570.

[25] J.Q. Meng, P.M. Oppeneer, J.A. Mydosh, P.S. Riseborough, K. Gofryk, J.J. Joyce, E.D. Bauer, Y. Li and T. Durakiewicz, Phys. Rev. Lett. 111 (2013) p.127002.

[26] See, for example, M. Tinkham, *Introduction to Superconductivity*, McGraw-Hill, New York, 1975.